Photocatalysis Hot Paper

How to cite: *Angew. Chem. Int. Ed.* **2023,** *62,* e202301815
International Edition: doi.org/10.1002/anie.202301815
German Edition: doi.org/10.1002/ange.202301815

Insights into the Role of Graphitic Carbon Nitride as a Photobase in Proton-Coupled Electron Transfer in (sp^3)C–H Oxygenation of Oxazolidinones

*Alexey Galushchinskiy[+], Yajun Zou[+], Jokotadeola Odutola, Pavle Nikačević, Jian-Wen Shi, Nikolai Tkachenko, Núria López, Pau Farràs, and Oleksandr Savateev**

Abstract: Graphitic carbon nitride (g-CN) is a transition metal free semiconductor that mediates a variety of photocatalytic reactions. Although photoinduced electron transfer is often postulated in the mechanism, proton-coupled electron transfer (PCET) is a more favorable pathway for substrates possessing X–H bonds. Upon excitation of an (sp^2)N-rich structure of g-CN with visible light, it behaves as a photobase—it undergoes reductive quenching accompanied by abstraction of a proton from a substrate. The results of modeling allowed us to identify active sites for PCET—the 'triangular pockets' on the edge facets of g-CN. We employ excited state PCET from the substrate to g-CN to selectively cleavethe *endo*-(sp^3)C–H bond in oxazolidine-2-ones followed by trapping the radical with O_2. This reaction affords 1,3-oxazolidine-2,4-diones. Measurement of the apparent pK_a value and modeling suggest that g-CN excited state can cleave X–H bonds that are characterized by bond dissociation free energy (BDFE) $\approx$100 kcal mol^{-1}.

Introduction

Oxidation and reduction of organic molecules based on single electron transfer (SET) can be designed by employing excited states of organic molecules,[1] transition metal complexes[2] and semiconductors,[3] which are collectively called 'photocatalysts'. SET reactions are energy demanding because they produce charged radical intermediates–cations and anions,[1] and require the excited state of the photocatalyst to be sufficiently oxidative and/or reductive. Redox reactions become facile when coupled with transfer of a proton—proton-coupled electron transfer (PCET, Figure 1a).[4] Unlike radical ions formed by SET, the products of PCET are electrically neutral radicals. The nature of PCET process makes the process more dependent on thermodynamic factors and kinetic behavior of a proton, including acid-base interaction between the substrate and the catalyst and tunneling effects, rather than on pure electrochemistry to lower the energy barriers for transition states.[5,6] In fact, the activation energy is sufficiently low to drive efficient enzyme-catalyzed biochemical redox processes at low temperature.[7,8]

In the last decade, effortless and selective modification of X–H sites in organic molecules by means of PCET driven by photoredox catalysis has attracted close attention.[9–11] By combining a sufficiently oxidative excited state of a molecular sensitizer, such as an Ir-polypyridine complex, with a Brønsted base, it is possible to cleave relatively strong N–H and O–H bonds in amides and phenols to generate alkoxy and amidyl radicals respectively via *oxidative* multisite PCET.[12,13] In water, a base/oxidant couple delivers the required amount of energy to be used for homolytic X–H bond cleavage in a substrate, formal bond dissociation free energy (FBDFE, kcal mol^{-1}), which is defined by the pK_a of

[*] A. Galushchinskiy,[+] Dr. Y. Zou,[+] Dr. O. Savateev
Department of Colloid Chemistry, Max Planck Institute of Colloids and Interfaces
Am Mühlenberg 1, 14476 Potsdam (Germany)
E-mail: oleksandr.savatieiev@mpikg.mpg.de

Dr. Y. Zou,[+] Dr. J.-W. Shi
State Key Laboratory of Electrical Insulation and Power Equipment, Center of Nanomaterials for Renewable Energy, School of Electrical Engineering, Xi'an Jiaotong University
Xi'an, 710049 (China)

J. Odutola, Prof. N. Tkachenko
Photonic compounds and Nanomaterials, Chemistry and Advanced material group, Tampere University (Finland)

P. Nikačević, Prof. N. López
Institut Català d'Investigació Química (ICIQ-CERCA), The Barcelona Institute of Science and Technology (BIST)
Avda. Països Catalans, 16, 43007 Tarragona (Spain)

P. Nikačević
Universitat Rovila i Virgili (URV)
Carrer de l'Escorxador, s/n, 43003 Tarragona (Spain)

Dr. P. Farràs
School of Biological and Chemical Sciences, Ryan Institute, University of Galway
Galway H91 CF50 (Ireland)

[+] These authors contributed equally to this work.

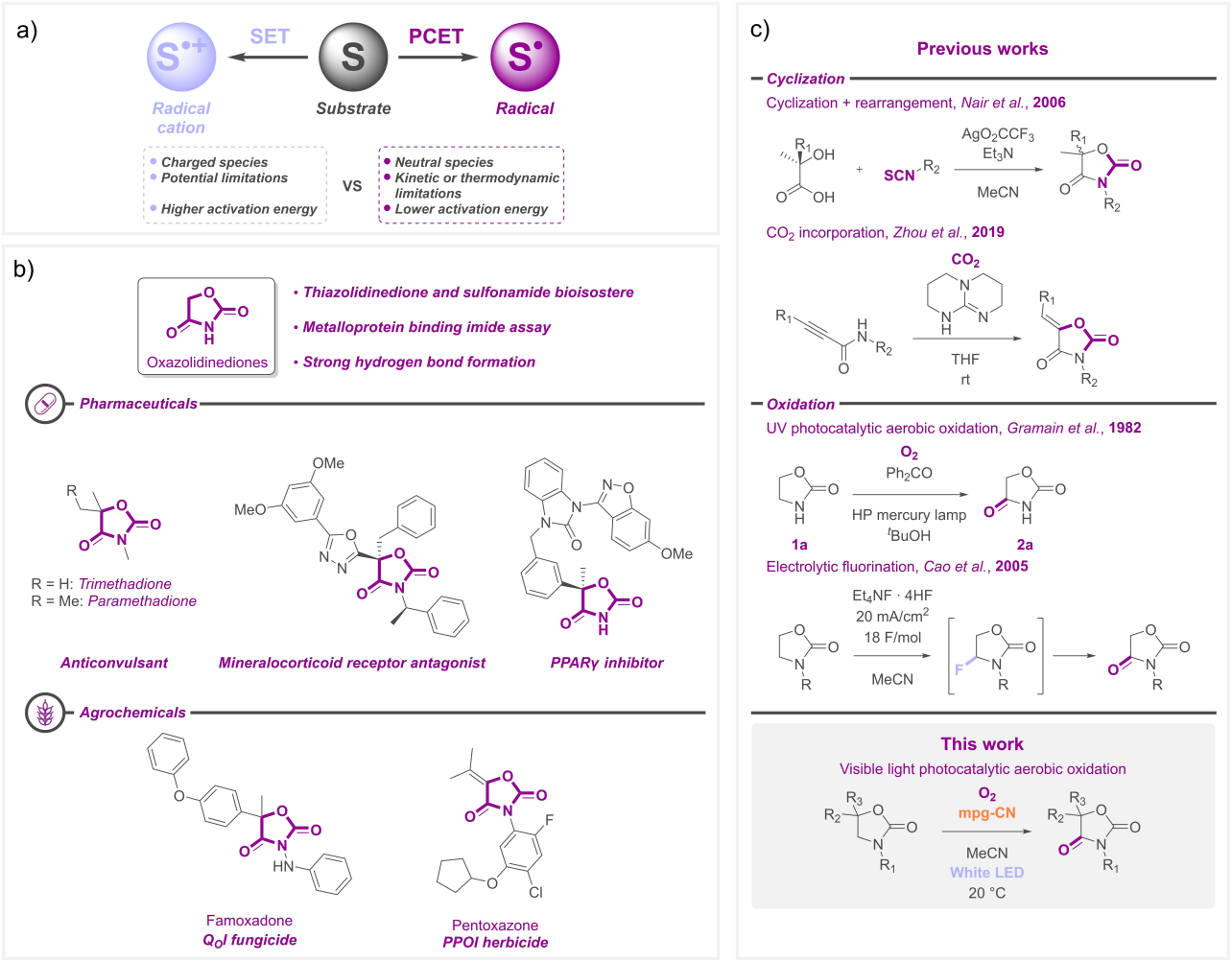

Figure 1. Concept of this article. a) Intermediates and features of oxidative SET and PCET catalytic pathways. b) Examples of biological activity of oxazolidinedione-containing molecules. c) Formation of 1,3-oxazolidine-2,4-diones reported in literature and in this work.

the acid conjugated to the Brønsted base and reduction potential of the sensitizer excited state (E^*_{red}, V vs. NHE):[4]

$$FBDFE = 1.37\mathrm{p}Ka + 23.06E^*_{red} + 57.6 \quad (1)$$

On the other hand, due to the presence of functional groups capable of acid-base interactions with a substrate molecule, the excited state of organic dyes, such as Eosin Y,[14] acts as hydrogen atom transfer (HAT) agent itself without adding an auxiliary base. Furthermore, inorganic semiconductors and oxoclusters are capable of engaging in PCET upon excitation with light.[15,16] The structure of heptazine-based graphitic carbon nitride (g-CN) is rich in pyridinic-like nitrogen centers.[17] Therefore, its excited state enables PCET from proton donors.[18–20] g-CN materials were postulated to mediate a number of reactions via PCET either explicitly or implicitly,[21,22] also in combination with organic bases. Related to conversion of organic molecules, cyanamide-modified carbon nitride with tributylmethylammonium dibutylphosphate as a base generates *N*-centered radical from carbamate, which undergoes intramolecular Giese addition to an allylic moiety.[23] Mesoporous g-CN (mpg-CN hereafter) in combination with $Br^{\bullet}$ produces an alkyl radical from *N*,*N*-dialkylformamide and enables the subsequent C–C cross coupling with arylhalides.[24] In combination with *N*-hydroxyphthalimide (NHPI), g-CN is used for oxygenation of allylic C–H bonds.[25] Our own results strongly suggest that ionic carbon nitride, potassium poly(heptazine imide) (K-PHI), is capable of abstracting electrons and protons from amines and store them as separated charges within the material.[26,27] The photocharged K-PHI is then used in *reductive* PCET to overcome high stability of otherwise non-reducible aryl halides and produce parent Ar–H compounds.[27]

Although the pK_a of protonated mpg-CN has not been reported, considering its nitrogen-rich structure, the valence band potential (E_{VB}) of +1.45 V vs. NHE and equation (1), we expect its excited state to be able to cleave C–H bonds, even those with moderate and relatively high BDFE. In particular, mpg-CN can oxidize *N*-alkyl amides, in which C–H BDFE is ≈89–94 kcal mol^{-1},[24] to their corresponding imides. An example of such a valuable imide moiety is 1,3-

oxazolidine-2,4-diones (Figure 1b, see discussion in the Supporting Information). Despite their high demand, the synthesis of 1,3-oxazolidine-2,4-diones remains challenging and inconvenient (Figure 1c). While the formation of 5-ylidene-substituted derivatives is achieved by base-catalyzed ring formation of propargylic amides with carbon dioxide,[28] regular oxazolidinediones usually require cyclization of a carbonate synthon, such as iso(thio)cyanates and α-hydroxycarboxylates,[29] which are not as readily available. An easier approach would be the oxidation of 1,3-oxazolidine-2-ones, which are either commercially available or conveniently prepared from the corresponding vicinal aminoalcohols, or by the reaction between oxiranes and isocyanates.[30] However, this pathway is not as easily achievable since oxazolidinones are quite stable against oxidation. A peak potential E_p >1.67–2.72 V vs. SCE was reported,[31] requiring strong oxidizers. Indeed, there are only two publications on successful oxidation of oxazolidinones at the 4th position of the ring. In 1982, Gramain et al. reported the photocatalytic reaction of oxazolidin-2-one **1a** with oxygen under irradiation with a high pressure mercury lamp using benzophenone as a catalyst over the course of 68 hours at room temperature.[32] In 2005, Gao et al. achieved electrolytic partial fluorination of *N*-substituted oxazolidinones, where non-acyl substituents yielded unstable 4-fluoro derivatives, which were then hydrolyzed and oxidized further to diones.[31] These methods involve rather harsh conditions, such as strong UV irradiation or corrosive acidic fluoride solutions.

Herein, we choose the synthesis of 1,3-oxazolidine-2,4-diones from the corresponding oxazolidinones to study PCET with mpg-CN upon band gap excitation. Due to dual function, organobase and a sensitizer, mpg-CN excited state cleaves selectively an endocyclic C–H bond in a β-position to the amide nitrogen followed by trapping of the intermediary C-centered radical with O_2. Experimental data as well as DFT simulations indicate that combination of mpg-CN surface basic character and the potential of the valence band allows to cleave X–H bonds with ≈100 kcal mol^{-1}.

Results and Discussion

Compound **1b** possesses *endo*- and *exo*-CH_2-groups. Therefore, it is a convenient platform to investigate selectivity of oxygenation. Secondary amides are usually oxidized more easily compared to tertiary amides due to the possibility of proton abstraction or its migration to oxygen.[33] In fact, some synthetic procedures rely mechanistically on the pathway of *N*-acylimine formation during oxidation.[34] Therefore, on the one hand, oxygenation of tertiary amides represents a synthetic challenge; on the other hand, the goal of the research is to establish a synthetic procedure suitable both for *N*-substituted and unsubstituted substrates.

The first round of screening involved testing of a series of heterogeneous carbon nitride photocatalysts prepared in our lab: mpg-CN,[35] potassium poly(heptazine imide) (K-PHI)[36] and sodium poly(heptazine imide) (Na-PHI).[37] The reaction was carried out under an oxygen atmosphere in acetonitrile under blue light irradiation (465 ± 10 nm). The highest yield of oxazolidinedione **2b** (25.5 % by qNMR with incomplete conversion of **1b**) was obtained with the mpg-CN photocatalyst (Table 1). mpg-CN also produces **2b** after three rounds of reuse (see Supporting Information for details).

K-PHI and Na-PHI gave **2b** with lower yields likely due to moderate surface area of a few tens of m^2 g^{-1}.[37,38] Molecular sensitizers, such as Riboflavin tetraacetate, Rhodamine B and Eosin Y gave **2b**, but with much lower yields, which nevertheless could be explained by the presence of carbonyl and/or carboxyl functionalities in their structure, which could enable PCET from **1b** in the absence of the external base. Indeed, the excited state of Eosin Y was identified as a direct HAT agent.[14] Although benzophenone was reported earlier to oxidize **1a**, likely due to interaction of amide NH with the photocatalyst C=O group, it failed to convert **1b**.[32] The excited states of Ir- and Ru-complexes are powerful SET agents, but in the absence of exogeneous base capable of engaging in multisite PCET they also failed to produce **2b**.[5] CdS and WO_3 did not give **2b** in significant quantity likely due to a lack of sufficient number of basic

Table 1: Screening for the optimal reaction conditions of oxazolidinone oxidation.[a]

Yield, %

Catalyst[b]		Light source[c]		Solvent[d]	
mpg-CN	25.5	UV LED (365 nm)	70.0	CH_3CN	55.5
K-PHI	21.0	Purple LED (410 nm)	14.5	MeOH	2.0
Na-PHI	7.5	Blue LED (465 nm)	25.5	EtOH	1.5
RFTA	1.0	Green LED (535 nm)	5.0	^{n}BuOH	5.0
Ir(ppy)$_3$	0.2	Red LED (625 nm)	0.5	^{t}BuOH	37.5
Ru(bpy)$_3$Cl$_2$ · 6H$_2$O	0.4	White LED	55.5	1,4-dioxane	1.5
Benzophenone	0.2	*No light*	0	Hexane	5.5
Methylene blue	0.2			Toluene	26.5
Rhodamine B	2.4			$CHCl_3$	13.5
Eosin Y	2.2			CH_2Cl_2	37.0
CdS	0.4			H_2O	22.5
WO_3	0.1			$MeNO_2$	45.0
mpg-CN (Ar, control)	2.8			DMSO	0
No catalyst	0[e]			DMF	0
No catalyst	10[f]				

[a] Reaction conditions: 0.05 mmol of **1b**, O_2 (1 bar), 2 mL of solvent (0.025 M), LED irradiation, catalyst: 5 mg (for heterogeneous, 100 g mol^{-1}), 5 mol.% (for homogeneous); yield values were obtained by quantitative ^{1}H NMR using 1,3,5-trimethoxybenzene as an internal standard. [b] the catalysts were screened using an optimal light source with respect to their absorption maxima, see Supporting Information for details; acetonitrile was used as a solvent. RFTA—riboflavin tetraacetate. [c] mpg-CN was used as a catalyst with acetonitrile as a solvent. [d] mpg-CN was used as a catalyst under white LED irradiation. [e] blue LED (465 nm). [f] UV LED (365 nm). Photon fluxes of LED sources: UV LED (365 nm) 0.2 μmol cm^{-2} s^{-1}; purple LED (410 nm) 0.4 μmol cm^{-2} s^{-1}; blue LED (465 nm) 0.8 μmol cm^{-2} s^{-1}; green LED (535 nm) 0.4 μmol cm^{-2} s^{-1}; red LED (625 nm) 1.6 μmol cm^{-2} s^{-1}.

sites on the surface that are capable to participate in the PCET. In Table 1, where the yield of **2b** is low, conversion of **1b** is also close to zero. Control experiment performed under Ar confirmed that oxygen is primarily transferred from air. The reaction did not proceed in the absence of mpg-CN and irradiation at 465 nm. However, irradiation at 365 nm in the absence of mpg-CN gave **2b** with 10 % yield (photochemical process). Illumination with white LED increased the yield of **2b** to 55.5 % after 24 h irradiation time, which is due to a substantial contribution of 450 nm photons in the LED emission spectrum (Figure S28). mpg-CN produced **2b** with the yield 70 % when excited at 365 nm. Assuming that 10 % of the yield is due to photochemical conversion of **1b** (without mpg-CN), the remaining 60 % constitutes the photocatalytic part of the yield, which is close to 56 % obtained upon mpg-CN excitation with white LED. Compared to other solvents (see Supporting Information), due to polarity, chemical stability and lack of reactive C–H bonds, acetonitrile is the most suitable solvent to perform oxygenation of oxazolidinone **1b** under white LED illumination.

With the established reaction conditions using mpg-CN as the catalyst and acetonitrile as solvent, the batch experiment was scaled up to 1.25 mmol of substrate, and the reaction was performed with a series of oxazolidinones **1a–o** (Figure 2). Due to low cost of UV photons, oxygenation of *N*-aryl substituted oxazolidinones, such as **1e**,**f**, may in principle be conducted without mpg-CN.[39] However, our goal was to *i*) establish a general protocol applicable for a large scope of substrates, i.e., those with aromatic groups as chromophores and without chromophores, and *ii*) investigate the role of mpg-CN as the photobase. Therefore, we opted for white LED without contribution of UV photons to avoid direct excitation of the substrates. The scope demonstrated almost quantitative yield for unsubstituted oxazolidinone **1a** and moderate to good yields for *N*-substituted derivatives **1b–k** with few exceptions. Electron rich groups, such as the 4-methoxyphenyl fragment in **1h** showed typical behavior of 4-methoxyphenyl (PMP) protecting group when attached to amine or amide functionality[40]—it is readily cleaved under the photocatalytic conditions. The product of **1h** oxygenation is a parent oxazolidinedione **2a**, while only a small amount of the target product **2h** was observed. In turn, substrates **1i** and **1j** bearing *O*- and *N*-benzyl fragments gave the corresponding benzoyl-substituted oxazolidinediones (**2ia** and **2ja**, respectively) as major products with minimal to no yield of the target product of ring oxygenation only, such as **2ic**. Additionally, a product of further oxidation **2jc** was observed, and benzoic acid, the product of benzoyl cleavage, was isolated. In case of 5,5-dimethylated substrates **1l–n**, the yields decreased significantly compared to the derivatives free of the substituent in the 5th position. The selectivity of the process is also lower due to competitive oxygenation of *endo*- and *exo*-CH_2-groups in **1m**. Earlier, it was reported that $Br^{\bullet}$ radical abstracts hydrogen in cyclic amides both from *endo*- and *exo*-CH_2-group with a higher preference for the former.[24] In our work, mpg-CN selectively abstracts the hydrogen atom from the *exo*-CH_2-group in all cases except for **1m**. However, when the substrate contains benzylic CH_2, the PCET at this site becomes facile, as illustrated by oxygenation of **1i** and **1j**. Introduction of a bulky and electron donating phenyl substituent into the 5th position, compound **1o**, reduced selectivity by promoting ring decomposition side reactions. Benzoic acid was obtained as the main product in this case.

Among non-photocatalytic oxidation procedures (Figure 3, see Supporting Information for procedures and references), only catalytic RuO_4/$NaIO_4$ process gave reasonable quantity of **2k** on comparable scale while still being inferior to our photocatalytic approach in terms of both yield and synthetic simplicity—ruthenium tetroxide is known to be a severely toxic reagent incompatible with a number of functional groups.[41]

The information provided by conditions screening and scope studies' results gave us initial hints on the exact reaction mechanism. There are three possible pathways (Figure 4): 1) reaction of a substrate with singlet oxygen, 2) direct oxidation of a substrate via photoinduced electron transfer (PET), and 3) generation of C-centered radical via PCET. In our case, the catalytic system does not include a sacrificial electron donor which could quench the photogenerated hole and therefore promote oxygen reduction to superoxide radical. Therefore, the only possibility for oxygen activation is formation of singlet oxygen by the energy transfer (EnT) pathway from the catalyst. Indeed, sensitization of $^1O_2$ by K-PHI and mpg-CN was reported.[42]

However, screening of other well-known efficient singlet oxygen generating catalysts, such as methylene blue, Eosin Y and Rhodamine B,[43] gave minimal amounts of the target oxazolidinedione, which serves as an evidence for exclusion of this pathway from further investigation. Additionally, the reaction was carried under an oxygen pressure ranging from 1 to 4 bars (Figure 5a). We observed negligible influence of oxygen concentration on the product yield, which further disproves the involvement of active oxygen species in the reaction mechanism. Nonetheless, $^1O_2$ may still be responsible for side reactions occurring in the system, since the conversion increases at a higher oxygen pressure (Figure 5a). Another hint for direct interaction between the substrate and the catalyst is the behavior of 5-substituted oxazolidinones, such as **1l–m**, in the reaction. The distribution and yield of products, especially clearly seen for **1m**, implies the existence of a certain steric hindrance factor, which decreases reaction efficiency. This factor should be negligible if a small molecule, $^1O_2$, were to attack the substrate. To prove or disprove the involvement of PET, cyclic voltammetry experiments were performed for substrates **1b**, **1d**, **1e** and **1h** to evaluate their oxidation potentials (Figure 5b, S5). An excellent agreement between the oxidation potential of **1d**, +1.58 V vs. SCE (at half peak), and that reported earlier, +1.67 V vs. SCE (peak),[31] was found. Overall, the four compounds demonstrate higher oxidation potentials ($\geq$ +1.26 V vs. SCE) than the potential of the photogenerated hole in mpg-CN (+1.20 V vs. SCE),[35] which unambiguously indicates that PET from oxazolidinones to mpg-CN is thermodynamically challenging. This fact excludes the second pathway and makes PCET the most likely mechanism of the reaction. Likewise, the

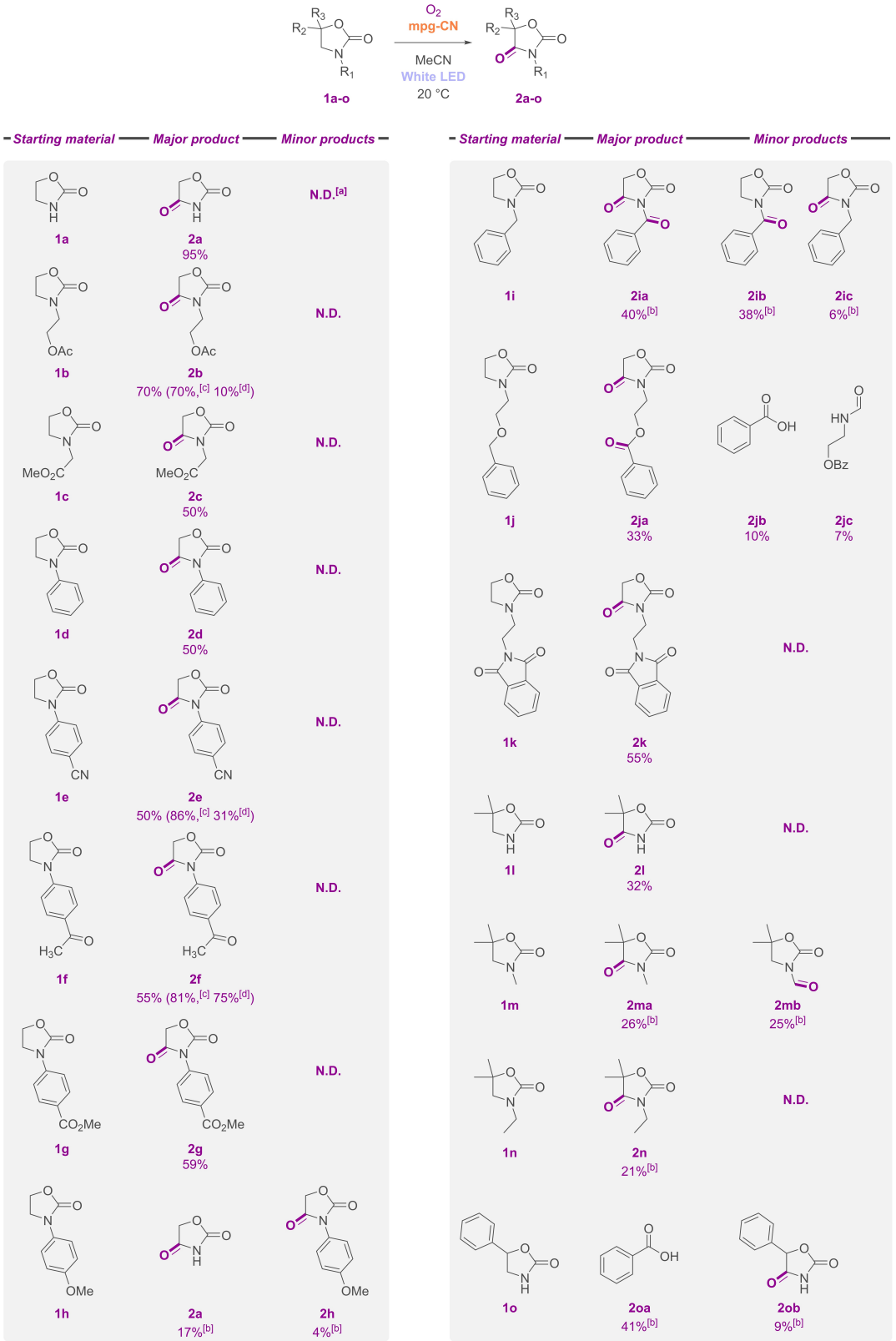

Figure 2. Scope of oxazolidinones **1a–o** used for scaled-up oxidation. Reaction conditions: **1** (1.25 mmol), O_2 (1 bar), acetonitrile (50 mL), mpg-CN (125 mg), white LED (4×50 W modules), 20 °C. The reaction was carried out until complete consumption of a starting material is achieved (24–72 h, monitored by ^{1}H NMR). Percent values indicate isolated yields unless stated otherwise. [a] "N.D." indicates absence of data for side products (either their formation was not observed by ^{1}H NMR or reaction mixture was too complex to distinguish minor components). [b] quantitative ^{1}H NMR yields using 1,3,5-trimethoxybenzene as an internal standard. [c] **1** (0.05 mmol), UV LED (365 nm). [d] **1** (0.05 mmol), UV LED (365 nm) without mpg-CN.

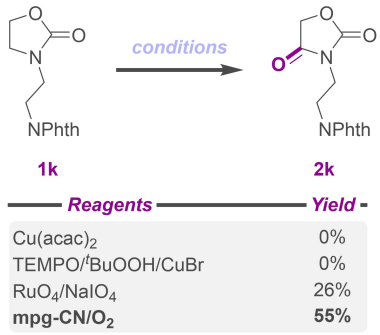

Figure 3. Comparison of the isolated yield of **2k** using different oxidation procedures.

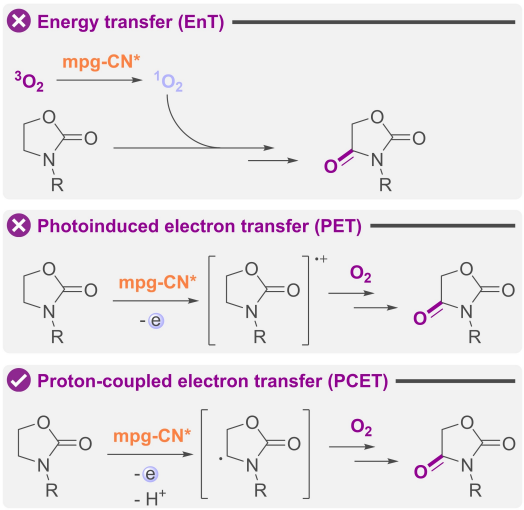

Figure 4. Simplified pathways of possible oxazolidinone oxidation mechanisms. Further steps regarding interaction with oxygen are omitted for clarity.

photocatalytic oxidation of oxazolidinone **1a** along with some lactams and hydantoins using benzophenone under UV is claimed to proceed via transfer of both proton and electron (Figure 1c).[32,44] We determined the apparent quantum yield (AQY) for oxidation of **1b** to be 0.026 % at 465 nm and 0.065 % at 365 nm excluding free-radical chain mechanism. Higher AQY obtained upon reaction mixture irradiation with UV light is explained by a higher extinction coefficient of mpg-CN.

From time resolved photoluminescence (tr-PL) spectroscopic measurements we conclude that while most of mpg-CN excited states decay rapidly, a small fraction survives for more than 400 µs after excitation (Figure 5c). In tr-PL spectra, fluorescence peak is observed at ≈472 nm (Figure 5d). The phosphorescence peak of lower intensity at ≈540 nm was measured by gating the emission from 40–100 µs with the pulsed xenon lamp. Singlet–triplet energy gap (ΔE_{ST}), determined as a difference between steady-state fluorescence and tr-PL maxima in Figure 5d, is 0.33 eV, which is consistent with the one reported earlier for K-PHI.[42,45] A relatively low ΔE_{ST} indicates that the triplet excited state has an energy comparable to the singlet and, in combination with the lifetime exceeding the µs range, we conclude that it is beneficial for the cleavage of C–H bond in oxazolidinones. The presence of the substrate **1b** and/or O_2 does not quench neither the singlet nor the triplet excited state of mpg-CN (Supporting Information Discussion 1). Transient absorption spectra of mpg-CN in MeCN recorded under anaerobic conditions are shown in Figure 5e. A few picoseconds after excitation, there was a strong negative signal between 500–750 nm which can be attributed to the ground state bleaching, and a positive signal between 850–1280 nm which can be attributed to the photogenerated excited state of mpg-CN. The crossing point was ≈800 nm. At a delay longer than 2 ns, the intensity of the positive signal reduced at a faster rate than the negative signal and the crossing point is redshifted to ≈1200 nm. On the nanosecond time scale, the behavior of mpg-CN excited state is similar to that of K-PHI[42] as indicated by the traces at 605, 960 and 1170 nm (Figure 5f). Similar to tr-PL study, TAS did not reveal differences in mpg-CN excited states' electronic signatures and dynamics, both singlet and triplet, on presence or absence of O_2 and **1b** (Supporting Information Discussion 1). We explain these observations by the low, 0.065 %, AQY of the studied reaction and the sensitivity of the instruments not high enough to detect this small quenching of mpg-CN excited states.

The reaction profile of **1b** oxidation by mpg-CN was rationalized by Density Functional Theory (DFT), as implemented in the Vienna Ab initio Simulation Package (VASP).[46] The carbon nitride was modeled as a six-heptazine-layer wide 2D surface with NH, NH_2, and OH groups at the termination sites,[24] and the reaction energy profile was obtained at the PBE level (Figure 6).[47]

All modeled structures were uploaded to the ioChem-BD database.[48] As mpg-CN is excited by light, the electrons from the valence band cross the band gap and enter the conduction band. Taking into account results of electron paramagnetic resonance spectroscopy study, hole and electron are separated by four heptazine units.[49] The calculated gap value of 2.6 eV (obtained with HSE06 a hybrid functional)[50] matches the experimental one, 2.7 eV, and explains the fact that among quasi-monochromatic light sources the reaction proceeds the most efficiently under the UV and blue LEDs (Table 1). Density of states (DOS) plot also confirms our CV results and demonstrates that highest occupied molecular orbital (HOMO) of oxazolidinone **1b** is significantly lower than the valence band of mpg-CN, indicating the impossibility of PET when it is not coupled with a proton transfer. As the oxazolidinone **1b** is oxidized, an electron and a proton are transferred from to the carbon nitride scaffold (PCET). This results in the formation of the oxazolidinone **1b** radical, **Int1**, as well as the hydrogenated carbon nitride radical [mpg-CN+H]•. Whether the [mpg-CN+H]• radical is formed in the excited state or directly in the ground state has little effect on the reaction energetics, as its Fermi level is close to the conduction band due to the extra electron present in the system (Figure S11). To assess the position of the additional H atom in the [mpg-CN+H]• system, an extensive search for the different positions was

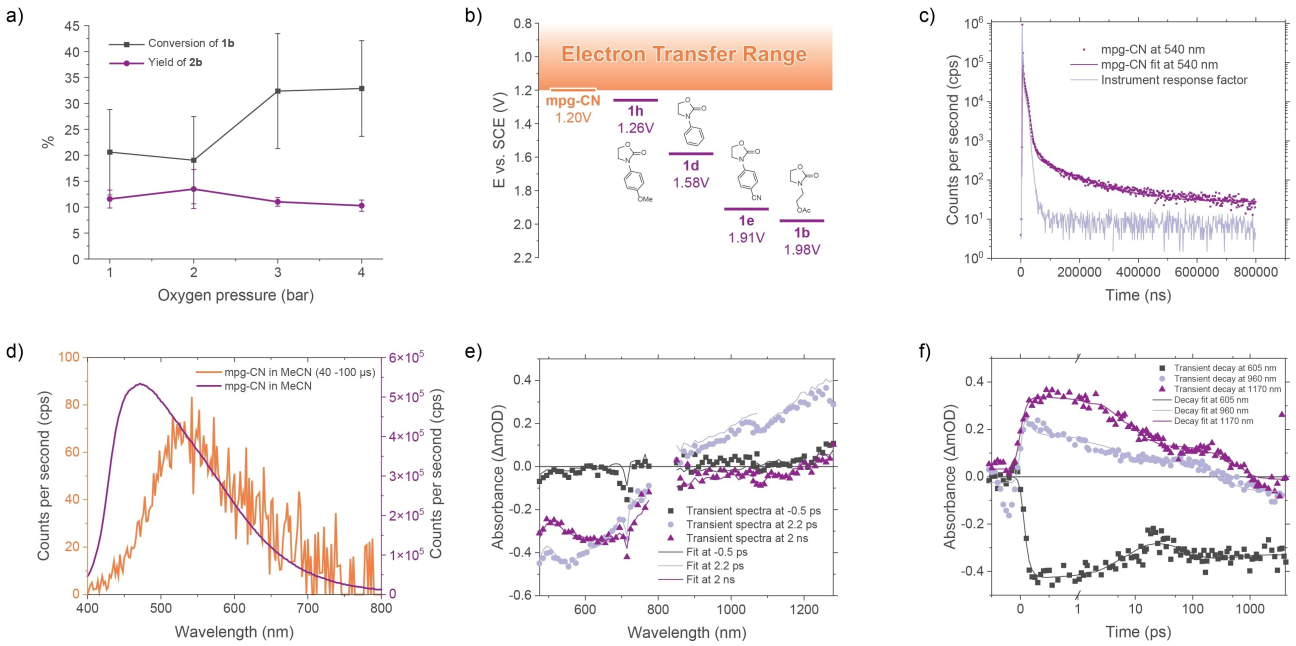

Figure 5. Investigation of oxazolidinone photocatalytic oxidation mechanism. a) Yield of **2b** and conversion of **1b** in the photocatalytic reaction performed under different oxygen pressures. Error bars represent average ± std ($n=3$). b) mpg-CN valence band potential and half-peak oxidation potentials of **1b**, **1d**, **1e** and **1h** with respect to SCE. Orange gradient band indicates the upper limit of potential range, where SET from a substrate to mpg-CN excited state is thermodynamically feasible. c) Tr-PL decay of mpg-CN and the IRF. d) Steady-state fluorescence (magenta) and tr-PL (orange) spectra of mpg-CN, the latter was measured by gating the emission from 40–100 µs with the pulsed xenon lamp. e) Transient absorption spectra of mpg-CN in MeCN under N_2. The spectra are cut off around 800 nm due to fundamental of the laser. f) Transient decay of mpg-CN in MeCN under N_2. The first picosecond is in linear scale while the rest has a logarithmic scale.

performed. We found that depending on the location of the hydrogen atom, the relative energy of the system spans over 3 eV (Figure S7). The lowest energy position of **Int1** ($\Delta E = +1.4$ eV) corresponds to the structure in which hydrogen atom is located inside the 'triangular pocket' and attached to the nitrogen atom of the heptazine unit. In the following step, the radical **Int1** traps oxygen molecule with the formation of a peroxo radical **Int2** ($\Delta E = -1.3$ eV). An alternative mechanistic pathway, according to which O_2 molecule captures the hydrogen atom from [mpg-CN+H]$^\bullet$ instead and forms the $HO_2^\bullet$ is by +0.4 eV uphill with the respect to **Int1** (Figure S9). Therefore, it is thermodynamically less favourable and can be discarded. The peroxo radical **Int2** recovers H-atom from [mpg-CN+H]$^\bullet$ and creates a hydroperoxide intermediate **Int3** ($\Delta E = -1.1$ eV), from which a water molecule is eliminated, and **2b** is produced ($\Delta E = -3.0$ eV).

In the absence of photoexcitation, the H-atom transfer from **1b** to carbon nitride would be the only non-spontaneous step. To make sure that the energy of this step is computed accurately, we also simulated the H-atom transfer to another proposed model of polymeric carbon nitride—melon-CN.[51] The melon model gave energies for the transfer within 0.3 eV of our mpg-CN model (Table S3), justifying the use of the mpg-CN model. We then proceeded to compute a more accurate electronic energy change for the H-atom transfer to mpg-CN using the HSE06 hybrid functional. After including the vibrational frequencies of adsorbates and gas-phase entropies, we determined the Gibbs free energy change of +1.5 eV for this step. This value is significantly smaller compared to *endo*-C–H BDFE in β-position to amide nitrogen in **1b** of 4.03 eV or 92.9 kcal mol^{-1} in vacuum. In other words, the intrinsically highly exergonic homolytic C–H bond cleavage becomes more facile when H-atom is transferred to mpg-CN.

In order to assess the range of X–H bonds that mpg-CN excited state may cleave homolytically, we measured the pK_a value of protonated mpg-CN in water, which is 6.60 ± 0.3. The heterogeneous material contains myriads of protonation sites that are different in their basicity. The obtained value should be considered as 'apparent' or 'average' pK_a value. Due to mutual electron-withdrawing effect of (sp^2)N atoms, the pK_a of bare heptazinium cation must be close to zero or even negative. However, the measured pK_a describes protonated mpg-CN as a weak acid. Such a discrepancy might be explained by the mutual effect of adjacent heptazine units that form a 'triangular pocket' and thus stabilize a proton similarly to a proton sponge. Using the obtained pK_a value and E_{VB} of +1.45 V vs. NHE,[35] according to the equation (1) we determine FBDFE to be 100 ± 0.4 kcal mol^{-1} or 4.32 ± 0.02 eV. In other words, upon mpg-CN band gap excitation, it is able to cleave X–H bonds with BDFE < 100 kcal mol^{-1} (Supporting Information Discussion 4).

Upon band gap excitation, carbon nitrides with even more positive potential of the valence band, such as that in K-PHI (+2.2 V vs. NHE),[52] and higher surface basicity (pK_a of the conjugated acid > 6.6), can cleave even stronger

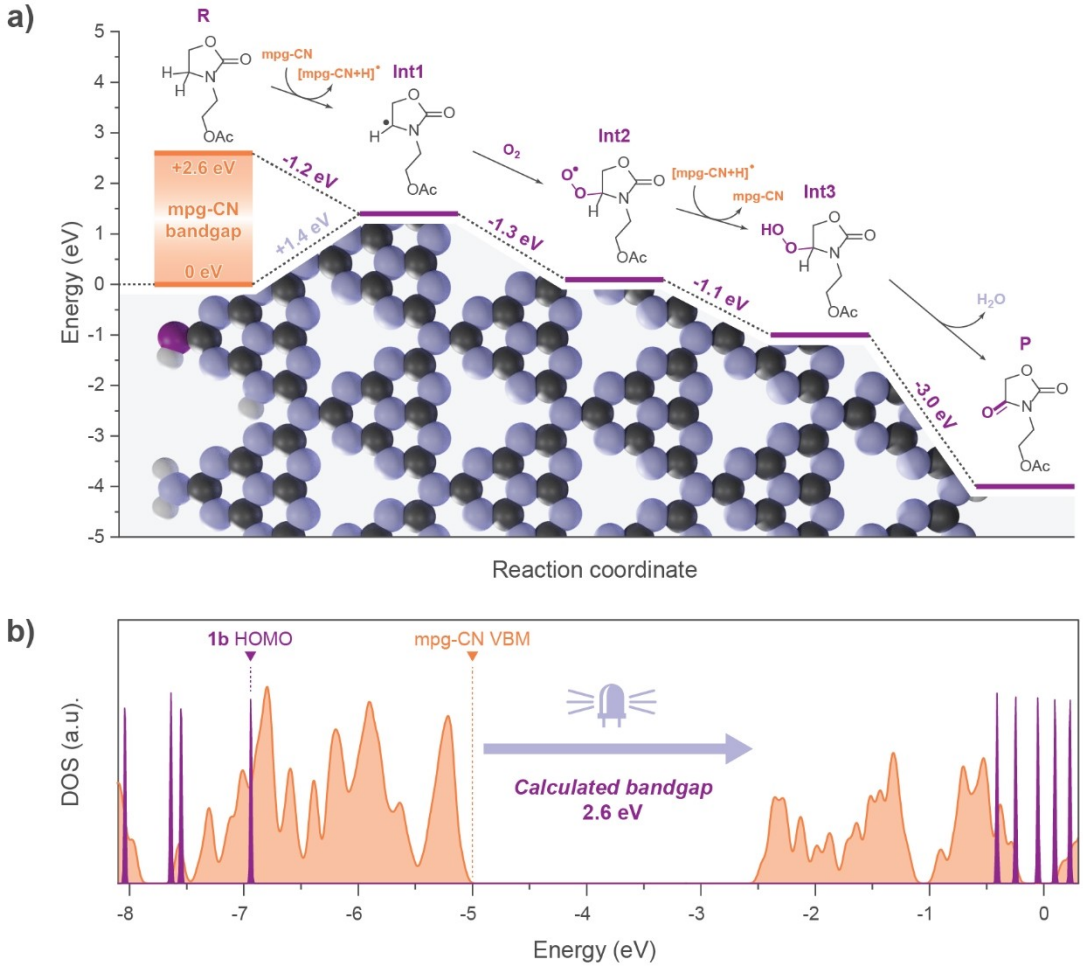

Figure 6. DFT results. a) Proposed mechanism for oxazolidinone **1b** oxidation at mpg-CN with potential energy differences of the respective intermediates. The mpg-CN + H model used in DFT calculations is shown in the lower part of the figure. The model contains NH, NH_2, and OH groups at the surface terminations, which is consistent with the experimental data.[24] b) DOS for mpg-CN (orange) and oxazolidinone **1b** (purple). The DFT energy scale corresponds to the energies obtained directly from the VASP output files. The correspondence between the two systems was confirmed by aligning the energies of oxygen 2 s electrons between these systems (not shown in the figure).

polar X–H bonds. By substituting pK_a and E_{VB} with these values in equation (1), we deduce that FBDFE >117.4 kcal mol^{-1}, which is close to O–H BDFE in water, 123 kcal mol^{-1}.[4] Indeed, K-PHI liberates O_2 from water upon illumination, when sacrificial electron acceptor effectively removes the photogenerated electrons from the conduction band.[38] In this work, K-PHI also demonstrates comparable and high activity in oxidation of **1b** (Table 1).

There are already many examples of photocatalytic reactions enabled by g-CNs that proceed via cleavage of C–H, O–H and N–H bonds with BDFE 80–123 kcal mol^{-1} (Table S4).[22,23,38,52–54] A basic environment is often required to facilitate cleavage of strong X–H bonds.[21,23] However, even without adding a base, mpg-CN, K-PHI and Na-PHI photocatalyze to some extent cleavage of O–H and N–H bonds in carboxylic acids and carbamates. A combination of the more basic character of the photocatalyst surface due to the presence of deprotonated imide moieties and the 0.7 V more positive potential of the valence band in ionic g-CNs compared to covalent g-CN is responsible for higher yields in oxidation of toluene to dibenzyldisulfide[52] and Minisci coupling.[22] Overall, the results summarized in Table S4 support our conclusions that g-CN materials serve as photobases to mediate an oxidative ES-PCET. Nevertheless, exogenous base is beneficial to suppress the transfer of a proton back to the intermediary radical and thus achieve higher yields in a chosen reaction.

As inferred from equation (1), high FBDFE required for the cleavage of strong X–H bonds may in principle be achieved by combining in one pot a superbase (large pK_a) and a strong oxidant (highly positive E_{red}). In practice, FBDFE values for base/oxidant couples are limited to 71–98 kcal mol^{-1}, as the superbases are electron rich and would simply react with strong oxidants.[55] Except for the pendant NH- and NH_2-groups, carbon nitrides are free of X–H bonds, which explains the high chemical stability of this class of photocatalysts. Overall, increasing the surface basicity, e.g., by deprotonated cyanamide moieties[56,57] and shifting E_{VB} to more positive values by incorporating electron-accepting moieties, are two strategies that may be employed

to design and synthesize semiconductor materials to perform X–H functionalization of organic compounds via excited state PCET.

Conclusion

We established an optimal photocatalytic method to convert oxazolidinones to their respective 2,4-diones using an inexpensive heterogeneous mpg-CN photocatalyst and oxygen gas as an oxidant on a mmol batch scale. The heterogeneous organophotocatalytic approach is superior compared to homogeneous photoredox catalysis and non-photocatalytic systems, such as RuO_4/$NaIO_4$, in terms of yield and convenience of handling the reagents. A number of evidences, including insensitivity of the product yield to O_2 pressure, high oxidation potential of oxazolidinones, +1.26…1.98 V vs. SCE and time-resolved spectroscopic data, unambiguously exclude SET and EnT pathways. DFT simulations suggest that the initial step, (sp^3)C–H bond cleavage in oxazolidinone via PCET, is uphill. mpg-CN as the organophotocatalyst makes it possible to overcome the energy barrier by converting the energy of the electromagnetic radiation into the driving force for PCET.

Acknowledgements

This project has received funding from the European Union's Horizon 2020 research and innovation programme under the Marie Skłodowska-Curie grant agreement No. 861151 Solar2Chem. The material presented and views expressed here are the responsibility of the authors only. The EU Commission takes no responsibility for any use made of the information set out. Olaf Niemeyer (the head of NMR facility of the MPICI), Michael Born (electric workshop of the MPICI), Cliff Janiszewski (glass blowing workshop of the MPICI) and Jan von Szada-Borryszkowski (mechanical workshop of the MPICI) are acknowledged for their contribution to this project. We thank BSC-RES for providing generous computational time. Open Access funding enabled and organized by Projekt DEAL.

Conflict of Interest

A patent WO/2019/081036 has been filed by Max Planck Gesellschaft zur Förderung der Wissenschaften E.V. in which O.S. is listed as a co-author.

Data Availability Statement

The data that support the findings of this study are available from the corresponding author upon reasonable request. The computed structures can be retrieved in the ioChem-BD database [48].

Keywords: Carbon Nitride · DFT · Oxazolidinone · PCET · Photocatalysis

[1] N. A. Romero, D. A. Nicewicz, *Chem. Rev.* **2016**, *116*, 10075–10166.
[2] C. K. Prier, D. A. Rankic, D. W. C. MacMillan, *Chem. Rev.* **2013**, *113*, 5322–5363.
[3] H. Kisch, *Angew. Chem. Int. Ed.* **2013**, *52*, 812–847; *Angew. Chem.* **2013**, *125*, 842–879.
[4] J. J. Warren, T. A. Tronic, J. M. Mayer, *Chem. Rev.* **2010**, *110*, 6961–7001.
[5] E. C. Gentry, R. R. Knowles, *Acc. Chem. Res.* **2016**, *49*, 1546–1556.
[6] C. Costentin, M. Robert, J.-M. Savéant, *Acc. Chem. Res.* **2010**, *43*, 1019–1029.
[7] R. Tyburski, T. Liu, S. D. Glover, L. Hammarstrom, *J. Am. Chem. Soc.* **2021**, *143*, 560–576.
[8] J. Bonin, M. Robert, *Photochem. Photobiol.* **2011**, *87*, 1190–1203.
[9] L. Capaldo, D. Ravelli, *Eur. J. Org. Chem.* **2017**, 2056–2071.
[10] L. Capaldo, D. Ravelli, M. Fagnoni, *Chem. Rev.* **2022**, *122*, 1875–1924.
[11] P. R. D. Murray, J. H. Cox, N. D. Chiappini, C. B. Roos, E. A. McLoughlin, B. G. Hejna, S. T. Nguyen, H. H. Ripberger, J. M. Ganley, E. Tsui, N. Y. Shin, B. Koronkiewicz, G. Qiu, R. R. Knowles, *Chem. Rev.* **2022**, *122*, 2017–2291.
[12] E. Tsui, A. J. Metrano, Y. Tsuchiya, R. R. Knowles, *Angew. Chem. Int. Ed.* **2020**, *59*, 11845–11849; *Angew. Chem.* **2020**, *132*, 11943–11947.
[13] C. B. Roos, J. Demaerel, D. E. Graff, R. R. Knowles, *J. Am. Chem. Soc.* **2020**, *142*, 5974–5979.
[14] X.-Z. Fan, J.-W. Rong, H.-L. Wu, Q. Zhou, H.-P. Deng, J. D. Tan, C.-W. Xue, L.-Z. Wu, H.-R. Tao, J. Wu, *Angew. Chem. Int. Ed.* **2018**, *57*, 8514–8518; *Angew. Chem.* **2018**, *130*, 8650–8654.
[15] C. Chen, T. Shi, W. Chang, J. Zhao, *ChemCatChem* **2015**, *7*, 724–731.
[16] G. Laudadio, Y. Deng, K. v. d. Wal, D. Ravelli, M. Nuño, M. Fagnoni, D. Guthrie, Y. Sun, T. Noël, *Science* **2020**, *369*, 92–96.
[17] A. Savateev, I. Ghosh, B. König, M. Antonietti, *Angew. Chem. Int. Ed.* **2018**, *57*, 15936–15947; *Angew. Chem.* **2018**, *130*, 16164–16176.
[18] E. J. Rabe, K. L. Corp, X. Huang, J. Ehrmaier, R. G. Flores, S. L. Estes, A. L. Sobolewski, W. Domcke, C. W. Schlenker, *J. Phys. Chem. C* **2019**, *123*, 29580–29588.
[19] K. L. Corp, E. J. Rabe, X. Huang, J. Ehrmaier, M. E. Kaiser, A. L. Sobolewski, W. Domcke, C. W. Schlenker, *J. Phys. Chem. C* **2020**, *124*, 9151–9160.
[20] D. Hwang, C. W. Schlenker, *Chem. Commun.* **2021**, *57*, 9330–9353.
[21] Q. Yang, G. Pan, J. Wei, W. Wang, Y. Tang, Y. Cai, *ACS Sustainable Chem. Eng.* **2021**, *9*, 2367–2377.
[22] A. Vijeta, E. Reisner, *Chem. Commun.* **2019**, *55*, 14007–14010.
[23] A. J. Rieth, Y. Qin, B. C. M. Martindale, D. G. Nocera, *J. Am. Chem. Soc.* **2021**, *143*, 4646–4652.
[24] S. Das, K. Murugesan, G. J. Villegas Rodríguez, J. Kaur, J. P. Barham, A. Savateev, M. Antonietti, B. König, *ACS Catal.* **2021**, *11*, 1593–1603.
[25] P. Zhang, Y. Wang, J. Yao, C. Wang, C. Yan, M. Antonietti, H. Li, *Adv. Synth. Catal.* **2011**, *353*, 1447–1451.
[26] Y. Markushyna, P. Lamagni, C. Teutloff, J. Catalano, N. Lock, G. Zhang, M. Antonietti, A. Savateev, *J. Mater. Chem. A* **2019**, *7*, 24771–24775.
[27] S. Mazzanti, C. Schritt, K. Brummelhuis, M. Antonietti, A. Savateev, *Exploration* **2021**, *1*, 20210063.

[28] H. Zhou, S. Mu, B.-H. Ren, R. Zhang, X.-B. Lu, *Green Chem.* **2019**, *21*, 991–994.
[29] a) V. A. Nair, S. M. Mustafa, M. L. Mohler, J. T. Dalton, D. D. Miller, *Tetrahedron Lett.* **2006**, *47*, 3953–3955; b) J. M. Cox, H. D. Chu, C. Yang, H. C. Shen, Z. Wu, J. Balsells, A. Crespo, P. Brown, B. Zamlynny, J. Wiltsie, J. Clemas, J. Gibson, L. Contino, J. Lisnock, G. Zhou, M. Garcia-Calvo, T. Bateman, L. Xu, X. Tong, M. Crook, P. Sinclair, *Bioorg. Med. Chem. Lett.* **2014**, *24*, 1681–1684.
[30] V. Yeh, R. Iyengar, *Comprehensive Heterocyclic Chemistry III*, Elsevier, Amsterdam, **2008**, pp. 487–543.
[31] Y. Cao, K. Suzuki, T. Tajima, T. Fuchigami, *Tetrahedron* **2005**, *61*, 6854–6859.
[32] J.-C. Gramain, R. Remuson, *J. Chem. Soc. Perkin Trans. 1* **1982**, 2341–2345.
[33] a) W. Huang, M. Wang, H. Yue, *Synthesis* **2008**, 1342–1344; b) S. Biswas, H. S. Khanna, Q. A. Nizami, D. R. Caldwell, K. T. Cavanaugh, A. R. Howell, S. Raman, S. L. Suib, P. Nandi, *Sci. Rep.* **2018**, *8*, 13649; c) J. Sperry, *Synthesis* **2011**, 3569–3580.
[34] a) K. C. Nicolaou, C. J. Mathison, *Angew. Chem. Int. Ed.* **2005**, *44*, 5992–5997; *Angew. Chem.* **2005**, *117*, 6146–6151; b) W. Lu, C. Mei, Y. Hu, *Synthesis* **2018**, *50*, 2999–3005.
[35] I. Ghosh, J. Khamrai, A. Savateev, N. Shlapakov, M. Antonietti, B. Konig, *Science* **2019**, *365*, 360–366.
[36] A. Savateev, D. Dontsova, B. Kurpil, M. Antonietti, *J. Catal.* **2017**, *350*, 203–211.
[37] Z. Chen, A. Savateev, S. Pronkin, V. Papaefthimiou, C. Wolff, M. G. Willinger, E. Willinger, D. Neher, M. Antonietti, D. Dontsova, *Adv. Mater.* **2017**, *29*, 1700555.
[38] A. Savateev, S. Pronkin, J. D. Epping, M. G. Willinger, C. Wolff, D. Neher, M. Antonietti, D. Dontsova, *ChemCatChem* **2017**, *9*, 167–174.
[39] M. Sender, D. Ziegenbalg, *Chem. Ing. Tech.* **2017**, *89*, 1159–1173.
[40] P. G. M. Wuts, *Greene's Protective Groups in Organic Synthesis*, 5th ed., Wiley, Hoboken, **2014**.
[41] V. S. Martín, J. M. Palazón, C. M. Rodríguez, C. R. Nevill, D. K. Hutchinson, *Encyclopedia of Reagents for Organic Synthesis*, Wiley, Hoboken, **2013**.
[42] A. Savateev, N. V. Tarakina, V. Strauss, T. Hussain, K. ten Brummelhuis, J. M. Sánchez Vadillo, Y. Markushyna, S. Mazzanti, A. P. Tyutyunnik, R. Walczak, M. Oschatz, D. M. Guldi, A. Karton, M. Antonietti, *Angew. Chem. Int. Ed.* **2020**, *59*, 15061–15068; *Angew. Chem.* **2020**, *132*, 15172–15180.
[43] a) Y. Zhang, C. Ye, S. Li, A. Ding, G. Gu, H. Guo, *RSC Adv.* **2017**, *7*, 13240–13243; b) F. Stracke, M. Heupel, E. Thiel, *J. Photochem. Photobiol. A* **1999**, *126*, 51–58.
[44] a) J.-C. Gramain, R. Remuson, Y. Troin, *J. Chem. Soc. Chem. Commun.* **1976**, 194–195; b) J.-C. Gramain, R. Remuson, Y. Troin, *Tetrahedron* **1979**, *35*, 759–765.
[45] A. Galushchinskiy, K. ten Brummelhuis, M. Antonietti, A. Savateev, *ChemPhotoChem* **2021**, *5*, 1020–1025.
[46] a) G. Kresse, J. Furthmuller, *Phys. Rev. B* **1996**, *54*, 11169–11186; b) G. Kresse, D. Joubert, *Phys. Rev. B* **1999**, *59*, 1758–1775.
[47] J. P. Perdew, K. Burke, M. Ernzerhof, *Phys. Rev. Lett.* **1996**, *77*, 3865–3868.
[48] P. Nikačević, **2023**, DOI: 10.19061/iochem-bd-1-249.
[49] A. Actis, M. Melchionna, G. Filippini, P. Fornasiero, M. Prato, E. Salvadori, M. Chiesa, *Angew. Chem. Int. Ed.* **2022**, *61*, e202210640; *Angew. Chem.* **2022**, *134*, e202210640.
[50] a) J. Heyd, G. E. Scuseria, M. Ernzerhof, *J. Chem. Phys.* **2003**, *118*, 8207–8215; b) J. Heyd, G. E. Scuseria, M. Ernzerhof, *J. Chem. Phys.* **2006**, *124*, 219906.
[51] V. W. Lau, B. V. Lotsch, *Adv. Energy Mater.* **2022**, *12*, 2101078.
[52] A. Savateev, B. Kurpil, A. Mishchenko, G. Zhang, M. Antonietti, *Chem. Sci.* **2018**, *9*, 3584–3591.
[53] T. Song, B. Zhou, G.-W. Peng, Q.-B. Zhang, L.-Z. Wu, Q. Liu, Y. Wang, *Chem. Eur. J.* **2014**, *20*, 678–682.
[54] Y. Cai, Y. Tang, L. Fan, Q. Lefebvre, H. Hou, M. Rueping, *ACS Catal.* **2018**, *8*, 9471–9476.
[55] C. R. Waidmann, A. J. M. Miller, C.-W. A. Ng, M. L. Scheuermann, T. R. Porter, T. A. Tronic, J. M. Mayer, *Energy Environ. Sci.* **2012**, *5*, 7771–7780.
[56] J. Kröger, F. Podjaski, G. Savasci, I. Moudrakovski, A. Jiménez-Solano, M. W. Terban, S. Bette, V. Duppel, M. Joos, A. Senocrate, R. Dinnebier, C. Ochsenfeld, B. V. Lotsch, *Adv. Mater.* **2022**, *34*, 2107061.
[57] I. F. Teixeira, N. V. Tarakina, I. F. Silva, N. López-Salas, A. Savateev, M. Antonietti, *Adv. Sustainable Syst.* **2022**, *6*, 2100429.

Manuscript received: February 6, 2023
Accepted manuscript online: February 28, 2023
Version of record online: March 28, 2023